

The *Caenorhabditis elegans* Muscle Specific Serpin, SRP-3, Neutralizes Chymotrypsin-like Serine Peptidases[†]

Stephen C. Pak,^{‡,§} Christopher Tsu,^{§,||} Cliff J. Luke,[‡] Yuko S. Askew,[‡] and Gary A. Silverman^{*,‡}

UPMC Newborn Medicine Program, Department of Pediatrics, University of Pittsburgh School of Medicine, Children's Hospital of Pittsburgh, and Magee-Womens Research Institute, Pittsburgh, Pennsylvania 15213, and Oncology Biochemistry, Millennium Pharmaceuticals, Inc., 40 Landsdowne Street, Cambridge, Massachusetts 02139

Received December 23, 2005; Revised Manuscript Received February 21, 2006

ABSTRACT: Members of the intracellular serpin family may help regulate apoptosis, tumor progression, and metastasis. However, their in vivo functions in the context of a whole organism have not been easily defined. To better understand the biology of these serpins, we initiated a comparative genomics study using *Caenorhabditis elegans* as a model organism. Previous in silico analysis suggested that the *C. elegans* genome harbors nine serpin-like sequences bearing significant similarities to the human clade B intracellular serpins. However, only five genes appear to encode full-length serpins with intact reactive site loops. To determine if this was the case, we have cloned and expressed a putative inhibitory-type *C. elegans* serpin, *srp-3*. Analysis of SRP-3 inhibitory activity indicated that SRP-3 was a potent inhibitor of the serine peptidases, chymotrypsin and cathepsin G. Spatial and temporal expression studies using GFP and *LacZ* promoter fusions indicated that SRP-3 was expressed primarily in the anterior body wall muscles, suggesting that it may play a role in muscle cell homeostasis. Combined with previous studies showing that SRP-2 is an inhibitor of the serine peptidase, granzyme B, and lysosomal cysteine peptidases, these data suggested that *C. elegans* expressed at least two inhibitory-type serpins with nonoverlapping expression and inhibitory profiles. Moreover, the profiles of these clade L serpins in *C. elegans* share significant similarities with the profiles of clade B intracellular serpin members in higher vertebrates. This degree of conservation suggests that *C. elegans* should prove to be a valuable resource in the study of metazoan intracellular serpin function.

Serpins¹ are key regulators in a multitude of biological processes that require precise control of peptide bond hydrolysis. This activity is most evident in the procoagulation, anticoagulation, and fibrinolytic cascades where plasma peptidases such as thrombin, protein C, and plasmin are tightly regulated by antithrombin III (SERPINC1), protein C inhibitor (SERPINA5), and plasminogen activator inhibitor type 1 (SERPINE1), respectively (reviewed in refs 1 and 2). Although many of the circulating serpins have been well characterized structurally, biochemically, and biologically,

humans and other vertebrate species also express an enigmatic subset of serpins whose functions are not well defined. This subset of serpins can be distinguished from other serpin family members by the lack of a cleavable N-terminal signal peptide, the absence of N- or C-terminal extensions, an inhibitory profile that targets serine and/or papain-like cysteine peptidases, and a cytosolic or nucleocytosolic subcellular distribution (reviewed in ref 3). These intracellular serpins (serpins_{IC}) are present also in all metazoan species examined to date. The broad distribution of serpins_{IC} provides an opportunity to study their function by comparative genomics using simpler model systems. To this end, we embarked upon studies to assess the activity of serpins_{IC} using the genetically tractable species *Caenorhabditis elegans*. The *C. elegans* genome encodes nine serpin_{IC} (*srp*) genes (4). However, only five of the *srp* genes (*srp-1*, -2, -3, -6, and -7) appear to encode peptidase inhibitory-type serpins, whereas the remaining genes encode transcripts without a reactive site loop (RSL) or premature termination codons that would activate mRNA decay or lead to synthesis of a truncated protein without an RSL (4). While in silico analysis is helpful in predicting the overall repertoire of serpins_{IC} in different species, these assessments are imperfect and require confirmation by experimentation. To date, only *srp-2* has been shown to encode a bona fide inhibitory-type serpin_{IC} in *C. elegans* (5). SRP-2 is a dual cross-class inhibitor and neutralizes granzyme B-like serine peptidases

[†] This work was supported by Grants CA87006 and CA86007 from the National Institutes of Health.

^{*} To whom correspondence should be addressed: UPMC Newborn Medicine Program, Department of Pediatrics, University of Pittsburgh School of Medicine, 300 Halket St., Pittsburgh, PA 15213. Telephone: (412) 641-4110. Fax: (412) 641-1844. E-mail: gsilverman@mail.magee.edu.

[‡] University of Pittsburgh School of Medicine, Children's Hospital of Pittsburgh, and Magee-Womens Research Institute.

[§] These authors contributed equally to this work.

^{||} Millennium Pharmaceuticals, Inc.

¹ Abbreviations: serpin, serine peptidase inhibitor; RSL, reactive site loop; cat, cathepsin; HNE, human neutrophil elastase; uPA, urokinase-type plasminogen activator; Succ-AAPF-pNA, succinyl-Ala-Ala-Pro-Phe-p-nitroanilide; MeO-Succ-AAPV-pNA, methoxy-Succ-Ala-Ala-Pro-Val-pNA; VLK-pNA, D-Val-Leu-Lys-pNA; EGR-pNA, H-Glu-Gly-Arg-pNA; (Z-FR)₂-R110, (Z-Phe-Arg)₂-R110; Z-K-SBzl, Z-Lys-thiobenzyl ester; DTD, dithiodipyridine; SI, stoichiometry of inhibition; MALDI-MS, matrix-associated laser desorption ionization mass spectroscopy.

and cathepsin L-like lysosomal cysteine peptidases and is expressed strongly in the hypodermal and intestinal cells of larval and adult worms. The goal of this study was to determine whether another putative inhibitory-type serpin_{IC}, *srp-3*, actually encodes a functional molecule that could participate in larval development or adult homeostasis. These studies showed that SRP-3 was a true inhibitory-type serpin that neutralized chymotrypsin-like serine peptidases that was expressed primarily in the anterior body wall muscles. This inhibitory activity confirmed that *C. elegans* expressed at least two functional serpins_{IC} whose expression patterns and inhibitory activity were shared with higher vertebrates.

EXPERIMENTAL PROCEDURES

cDNA Isolation. First-strand cDNA was prepared from total *C. elegans* RNA using Superscript II RNase H⁻ reverse transcriptase (Invitrogen, Carlsbad, CA). The full-length *srp-3* cDNA containing the putative open reading frame was amplified using sense (5'-ATCGCGGATCCATGTTTGACGTGGCAGAGCGTC-3') and (5'-ATCCGCTCGAGTTAAATTCAACCATTGAAAACCCCTAC-3') antisense primers. Primers were designed with *Bam*HI and *Xho*I restriction endonuclease recognition sites (underlined in the primer sequences) to simplify cloning and facilitate in-frame insertion into a bacterial protein expression vector (see below). The resulting PCR fragment (~1.1 kb) was subcloned into the pBluescript II KS (pBS) (Stratagene, La Jolla, CA) vector and sequenced.

Construction of Glutathione S-Transferase (GST) Fusion Proteins. To generate the bacterial expression plasmid, the full-length *srp-3* coding sequence was released from pBS by digestion with the restriction endonucleases, *Bam*HI and *Xho*I. The 1.1 kb insert was gel purified and ligated into the corresponding sites of the pGEX-6P-1 vector (Amersham Biosciences, Piscataway, NJ). DNA from the recombinant clone was sequenced to confirm in-frame insertion of intact *srp-3* DNA.

Purification of the GST-SRP-3 Fusion Protein. The GST-SRP-3 fusion protein was batch purified using glutathione-Sepharose 4B beads (Amersham Biosciences) as previously described (5).

Enzymes, Inhibitors, and Substrates. Human cathepsins (cat) G, L, and S; human chymotrypsin (CT); human neutrophil elastase (HNE); human pancreatic trypsin; and human plasmin were purchased from Athens Research and Technology Inc. (Athens, GA). CatK was a kind gift from D. Bromme (Department of Biochemistry and Molecular Biology, University of British Columbia, Vancouver, BC). Papain was purchased from Roche Applied Science (Indianapolis, IN). Subtilisin A and urokinase-type plasminogen activator (u-PA) were purchased from Sigma Chemical Co. (St. Louis, MO).

The serine and cysteine peptidase active site inhibitors, phenylmethanesulfonyl fluoride (PMSF) and *trans*-epoxysuccinyl-L-leucylamido(4-guanidino)butane (E64), respectively, were purchased from Sigma.

Enzyme substrates were purchased from Sigma [succinyl-Ala-Ala-Pro-Phe-*p*-nitroanilide (Succ-AAPF-*p*NA), methoxy-Succ-Ala-Ala-Pro-Val-*p*NA (MeO-Succ-AAPV-*p*NA), D-Val-Leu-Lys-*p*NA (VLK-*p*NA), Z-Lys-thiobenzyl ester (Z-K-SBzl), and dithiodipyridine (DTDP)], Bachem Bioscience,

Inc. (King of Prussia, PA) [H-Glu-Gly-Arg-*p*NA (EGR-*p*NA)], and Molecular Probes, Inc. (Eugene, OR) {(Z-Phe-Arg)₂-R110 [(Z-FR)₂-R110]}.

PBS [10 mM phosphate buffer, 27 mM KCl, and 137 mM NaCl (pH 7.4)] was used in enzymatic reactions with trypsin, plasmin, HNE, chymotrypsin, subtilisin A, and uPA. Cathepsin reaction buffer [50 mM sodium acetate (pH 5.5), 4 mM dithiothreitol, and 1 mM EDTA] was used with papain and catK, -L, and -S. A unique reaction buffer was used with catG [50 mM HEPES, 150 mM NaCl, and 5% *N,N*-dimethylformamide (pH 7.4)].

Thermal Stability Assay. Aliquots of recombinant GST-SRP-3 protein (final concentration of 0.5 mg/mL) were incubated for 7 min at temperatures ranging from 25 to 75 °C. The solution was placed on ice for 1 min and centrifuged (12000g for 10 min at 4 °C), and the supernatant was analyzed by SDS-PAGE.

Determination of Enzyme and Inhibitor Concentrations. Chymotrypsin was calibrated using 4-methylumbelliferyl-*p*-trimethylammoniocinnamate (Sigma) as previously described (6). Active site titration was performed using a fluorescence spectrophotometer (F-3010, Hitachi Instruments Inc., San Jose, CA) with a band-pass of 10 nm and excitation and emission wavelengths of 360 and 450 nm, respectively. Assays were performed in PBS, and the activity of the peptidase was determined by calibration with a standard curve of 4-methylumbelliferone (Sigma). CatG was calibrated with antichymotrypsin that was active site titrated against calibrated chymotrypsin. Activities of the cysteine peptidases (catK, -L, and -S) were determined by active site titration using E64 as described previously (7). The concentration of recombinant SRP-3 was determined by thermal denaturation and Bradford analysis (Protein Assay Kit II, Bio-Rad, Hercules, CA).

Assays for Inhibition. Peptidase inhibitory activity of SRP-3 was determined by mixing enzyme and inhibitor in the appropriate buffer, incubating for 15 min at 25 °C, and measuring residual enzyme activity as previously described (8). Residual enzyme activity was determined by assessing substrate hydrolysis over time (velocity) using either a THERMOMax (in the case of -*p*NA and -SBzl substrates) or an fmax (in the case of -R110 substrates) microplate reader (Molecular Devices, Sunnyvale, CA). For the UV-visible substrates, -*p*NA and -SBzl, wavelengths of 405 and 340 nm were used, respectively. For the fluorescent substrate, -R110, the excitation and emission spectra were recorded at 485 and 538 nm, respectively. The concentrations of enzyme, inhibitor, and substrate are listed in Table 1, and the buffers are listed above. Percent enzyme inhibition = 100 × (1 - velocity of inhibited enzyme reaction/velocity of uninhibited enzyme reaction).

Complex Formation. SRP-3-chymotrypsin complexes were formed by incubating 10 μg of GST-SRP-3 protein with 1 μg of chymotrypsin in PBS for 30 min at 25 °C. SRP-3-catG complexes were formed by incubating 10 μg of GST-SRP-3 protein with 1 μg of catG in catG buffer for 30 min at 25 °C. The mixture components were separated by SDS-PAGE, and higher-molecular weight protein bands were visualized following staining with Coomassie Brilliant Blue R-250.

Binding Stoichiometries. Assays for binding between SRP-3 and chymotrypsin or catG were performed in a

Table 1: Inhibitory Profile of SRP-3

proteinase (final concentration)	[SRP-3] (nM)	ratio ([I]/[E])	% inhibition	substrate (final concentration)
cathepsin G (50 nM)	500	10	100	Succ-AAPF-pNA (1 mM)
cathepsin K (20 nM)	200	10	0	(Z-FR) ₂ -R110 (5 μ M)
cathepsin L (20 nM)	200	10	0	(Z-FR) ₂ -R110 (5 μ M)
cathepsin S (50 nM)	500	10	0	(Z-FR) ₂ -R110 (5 μ M)
chymotrypsin (50 nM)	500	10	100	Succ-AAPF-pNA (1 mM)
human neutrophil elastase (50 nM)	500	10	85	MeO-Succ-AAPV-pNA (0.5 mM)
papain (50 nM)	500	10	0	(Z-FR) ₂ -R110 (5 μ M)
plasmin (50 nM)	500	10	0	VLK-pNA (0.1 mM)
subtilisin A (25 nM)	500	20	97	Succ-AAPF-pNA (1 mM)
trypsin (50 nM)	500	10	0	EGR-pNA (0.5 mM)
uPA (50 nM)	500	10	0	EGR-pNA (0.1 mM)

volume of 100 μ L in 96-well microtiter plates (EIA/RIA plates, Costar, Cambridge, MA). The inhibitor, SRP-3 (concentration range of 0–500 nM), was incubated with the enzyme, chymotrypsin (500 nM) or catG (50 nM), for 15 min at 25 °C. The substrate, Succ-AAPF-pNA, was added to a final concentration of 1 mM. The velocity of substrate hydrolysis was measured using the *THERMO*max microplate reader. The partitioning ratio of the inhibitor–enzyme association was determined by plotting the fractional activity (velocity of the inhibited enzyme reaction/velocity of the uninhibited enzyme reaction) versus the initial ratio of the inhibitor to enzyme (I_0/E_0) (7). The x -intercept [i.e., the stoichiometry of inhibition (SI)] was determined by linear regression analysis.

Enzyme Kinetics. The interaction of SRP-3 with chymotrypsin was assessed by the progress curve method (9). Under these pseudo-first-order conditions, a constant amount of enzyme (10 nM) was mixed with different concentrations of inhibitor (0–640 nM) and substrate (final concentration of 1 mM). The rate of product formation was measured using the *THERMO*max microplate reader. The K_m of chymotrypsin for Succ-AAPF-pNA in PBS was 345 μ M.

The association rate constant for the interaction of SRP-3 with catG was determined under second-order conditions (10, 11). Equimolar amounts of SRP-3 and catG were incubated at 25 °C for varying periods of time (0–30 min). The reaction was stopped by the addition of substrate (1 mM Z-Lys-SBzl and 250 μ M DTDP), and the velocity of free catG was measured using the *THERMO*max microplate reader. Velocity was converted to free enzyme concentration using an enzyme concentration standard curve. The rate of change in the amount of free enzyme over time is described below, where the slope of the reciprocal remaining free enzyme ($1/E_t$) over time (t) yields a second-order rate constant (k_a).

$$1/E_t = k_a t + 1/E_0$$

The y -intercept of this plot is the reciprocal of initial enzyme concentration (E_0).

Matrix-Associated Laser Desorption Ionization Mass Spectroscopy (MALDI-MS). Chymotrypsin (1 μ g) or catG (1 μ g) was mixed with SRP-3 (30 μ g) in the appropriate buffer (20 μ L) for 15 min at 25 °C. The mixture components were separated by MALDI-MS at the Wistar Protein Microchemistry Facility (Philadelphia, PA).

Worm Strain and Culture Conditions. The wild-type worm strain used in this study was *C. elegans* Bristol (N2). Worms were routinely cultured at 25 °C on standard nematode

growth medium (NGM) agar plates (12) seeded with *Escherichia coli* strain OP50 [Caenorhabditis Genetics Center (CGC), <http://biosci.umn.edu/CGC/CGChomepage.htm>].

Generation of *srp-3* Expression Constructs. A translational *srp-3::lacZ* fusion gene was made by ligating a 3.9 kb genomic fragment, containing the full-length *srp-3* gene and 2.2 kb of the upstream promoter sequence, in-frame into the *lacZ* pPD95.10 expression vector (a kind gift from A. Fire, Stanford University, Stanford, CA). To obtain germline expression, the recombinant transgene and a marker plasmid (*myo-3::gfp*) were co-microinjected into the gonads of adult hermaphrodites at final concentrations of 100 and 50 ng/ μ L, respectively. Transgenic animals were identified by selecting GFP-positive worms. *lacZ* expression was visualized by staining fixed worms with X-gal as previously described (13). To verify the SRP-3::*lacZ* expression pattern, a *srp-3::gfp* translational fusion was generated by ligating a 3.9 kb genomic fragment, containing the full-length *srp-3* gene and 2.2 kb of the upstream promoter sequence, in-frame into the *gfp* pPD95.81 expression vector (a kind gift from A. Fire). Transgenic worms were generated by co-injecting 20 ng/ μ L *srp-3::gfp* and 90 ng/ μ L pCeh361 (*dpy-5* rescue construct) into a *dpy-5* homozygous mutant (CB907) (14). Rescued wild-type worms were selected and observed for GFP expression.

RESULTS

Biochemical Characterization of SRP-3. Serpins, in their active conformation, are metastable and sensitive to denaturation and precipitation at elevated temperatures (>60 °C). In contrast, serpins in the latent conformation or those with a cleaved RSL are stable even upon incubation at temperatures of ≥ 100 °C. To test whether SRP-3 encoded a functional, inhibitory-type serpin, we prepared recombinant GST–SRP-3 fusion proteins using an *E. coli* expression system and performed a thermal denaturation assay. Recombinant SRP-3 was stable between 25 and 45 °C; however, at ≥ 55 °C, the serpin completely precipitated from solution (Figure 1). This result suggested that the recombinant SRP-3 protein was in the active conformation and could be used in peptidase inhibition assays.

The putative reactive center (P2–P2') of SRP-3, Pro-Met-Ser-Ala, bears remarkable similarity to that of human $\alpha 1$ -antitrypsin (SERPINA1), Pro-Met-Ser-Ile (Figure 2). This similarity suggested that SRP-3 might have an inhibitory profile comparable to that of $\alpha 1$ -antitrypsin. However, the inhibitory activity of a serpin cannot be ascertained by examination of the amino acid sequence alone and thus must

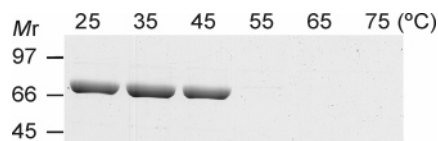


FIGURE 1: Thermal denaturation profile of SRP-3. Aliquots (5 μ g) of purified, recombinant GST–SRP-3 protein were incubated for 7 min at the temperatures indicated above the lanes. Each sample was chilled on ice for 1 min and centrifuged for 10 min. Supernatants were analyzed by SDS–PAGE, and protein bands were visualized by staining with Coomassie Brilliant Blue R-250.

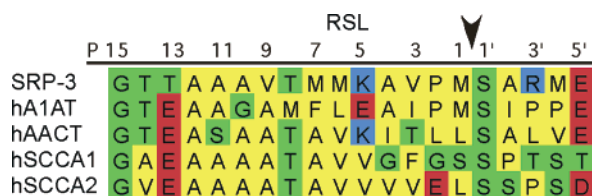


FIGURE 2: Amino acid alignment of *C. elegans* SRP-3 with human serpins. The amino acid sequence alignment was performed using ClustalW version 1.8 and SeqVu version 1.01 (J. Gardner, Garvan Institute of Medical Research, Sydney, Australia). Colors indicate polar (green), nonpolar and hydrophobic (yellow), acidic (red), and basic (blue) residues. The RSL is underlined and numbered from P15 to P5'. The putative scissile bond is marked by an arrowhead.

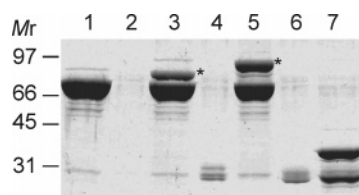


FIGURE 3: SRP-3–peptidase complexes. Enzyme, serpin, or serpin and enzyme were incubated at 25 °C for 10 min. Gel loading buffer (2 \times) was added, and each sample was heated to 95 °C for 5 min, and the proteins were separated by SDS–PAGE. Protein bands were visualized by staining with Coomassie Brilliant Blue R-250: lane 1, GST–SRP-3 protein alone (10 μ g); lane 2, chymotrypsin alone (1 μ g); lane 3, GST–SRP-3 protein (10 μ g) with chymotrypsin (1 μ g); lane 4, catG alone (1 μ g); lane 5, GST–SRP-3 protein (10 μ g) with catG (1 μ g); lane 6, human neutrophil elastase (HNE) alone (1 μ g); and lane 7, GST–SRP-3 protein (10 μ g) with HNE (1 μ g). GST–SRP-3–peptidase complexes are denoted with asterisks.

be determined experimentally. To this end, we tested SRP-3 inhibitory activity against a representative panel of serine and cysteine peptidases (Table 1). SRP-3 inhibited completely the enzymatic activities of human cathepsin (cat) G and chymotrypsin but showed no inhibitory activity against other serine peptidases, such as trypsin, plasmin, and urokinase-type plasminogen activator. SRP-3 also exhibited no inhibitory activity against the cysteine peptidases, papain and catK, -L, and -S. Modest inhibitory activity was observed against human neutrophil elastase and subtilisin A. However, subsequent SDS–PAGE analysis showed that the apparent inhibition observed with these enzymes was due to a simple competition reaction between SRP-3 and the reporter substrate (data not shown and Figure 3).

Once binding and cleavage have taken place at the reactive site loop (RSL), serpins form covalent acyl complexes with their target peptidases. These complexes are resistant to denaturation by heating in SDS buffers. To determine whether the GST–SRP-3 fusion protein forms a covalent complex with catG or chymotrypsin, we incubated the serpin with either peptidase for 5 min at room temperature.

Following the addition of the SDS sample buffer, the mixture was heated to 95 °C for 5 min. Samples were fractionated by SDS–PAGE under reducing conditions, and protein bands were visualized by staining with Coomassie Brilliant Blue R-250. A slow-migrating band representing a serpin–peptidase complex was visible when SRP-3 was incubated with chymotrypsin (Figure 3, lane 3) or catG (Figure 3, lane 5). No higher-molecular weight complexes were visible when SRP-3 was incubated with human neutrophil elastase. In contrast, SRP-3 was degraded by elastase, which confirmed that this serpin served as a substrate for this serine peptidase (Figure 3, lane 7).

The SI for the interaction between SRP-3 and catG (or chymotrypsin) was determined by incubating a constant amount of enzyme (E_0) with different concentrations of inhibitor (I_0) and plotting the fractional enzyme activity against I_0/E_0 . The I_0/E_0 ratio that results in the complete inactivation of the enzyme is the SI. The SIs for the interaction between SRP-3 and catG and between SRP-3 and chymotrypsin were ~ 1 and ~ 1.2 , respectively (Figure 4A,B). SIs near unity are typical of serpin–target peptidase interactions (15).

To determine the rate of formation of a complex of SRP-3 and catG, we measured the second-order rate constants (k_a) under second-order conditions (10). Equimolar amounts of SRP-3 and catG were incubated at 25 °C for varying periods of time (0–30 min). The reaction was stopped by the addition of substrate (1 mM Z-Lys-SBzl and 250 μ M DTDP), and the velocity of free catG was measured. Velocity was converted to free enzyme concentration using an enzyme concentration standard curve. The k_a value for the interaction of SRP-3 with catG was $\sim 1.3 \times 10^5 \text{ M}^{-1} \text{ s}^{-1}$ (Figure 4C).

Due to an SI of >1 , the interaction of SRP-3 and chymotrypsin was assessed under pseudo-first-order conditions using the progress method (7). The assay was performed by incubating 10 nM enzyme with various excess concentrations (0–640 nM) of inhibitor in the presence of 1 mM Succ-AAPF-pNA substrate. The progress of enzyme inactivation was followed, and the k_a was calculated by nonlinear regression analysis. The k_a value for the interaction of SRP-3 with chymotrypsin was $\sim 0.7 \times 10^5 \text{ M}^{-1} \text{ s}^{-1}$ (Figure 4D). These second-order rate constants are characteristic of physiologic interactions between serpins and their target peptidases (15).

Reactive Center of SRP-3. Cleavage of the serpin RSL by its target peptidase yields an ~ 4 kDa C-terminal fragment. By determining the exact molecular mass of the cleavage fragment, we were able to pinpoint the serpin reactive center (P1–P1'). The GST–SRP-3 fusion protein was incubated with catG or chymotrypsin, and the resulting C-terminal fragments were analyzed by MALDI-MS. In both cases, a major peak at $\sim 3915 \pm 1$ Da that matched the molecular mass of the SRP-3 peptide sequence, SARMEQPV.....IFVGVFNG, was detected (Figure 5A,B). This finding confirmed that the Met-Ser residues served as the reactive center (P1–P1') for the interaction of SRP-3 with both catG and chymotrypsin (Figure 5C).

Spatial and Temporal Expression of SRP-3. In addition to determining its biochemical activity, we also sought to determine the expression pattern of SRP-3. A translational *srp-3::LacZ* fusion gene was generated by ligating a 3.9 kb genomic fragment, containing the full-length *srp-3* gene and

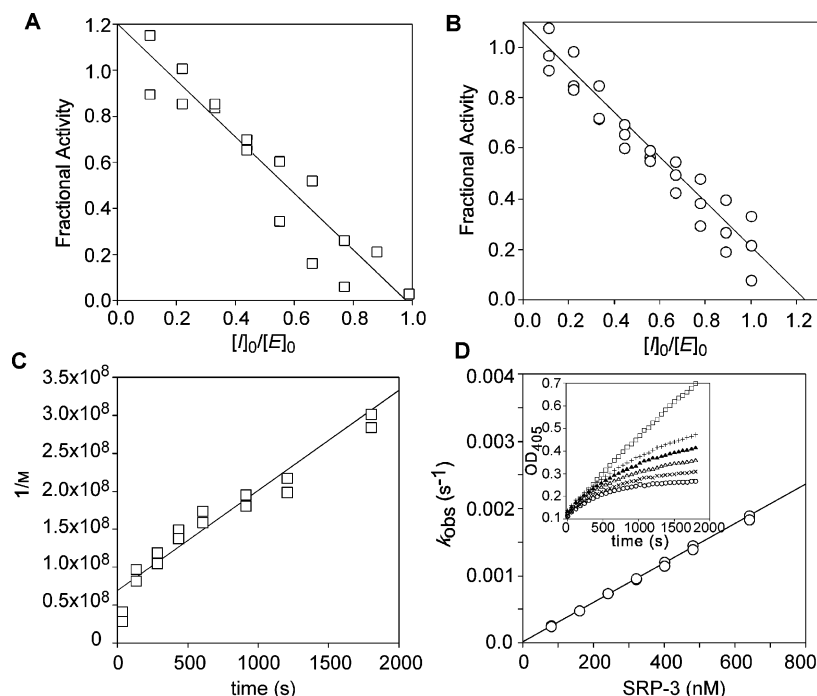


FIGURE 4: Kinetic analysis of the interaction between SRP-3 and target peptidases. (A and B) Stoichiometry of inhibition. Human catG (50 nM) (A) or chymotrypsin (500 nM) (B) was incubated with different concentrations of SRP-3 (0–500 nM) at 25 °C for 15 min. Residual catG and chymotrypsin activities were measured by adding the appropriate substrate and measuring the change in absorbance. The fractional activity was the ratio of the velocity of inhibited enzyme (v_i) to the velocity of uninhibited control (v_o). The stoichiometry of inhibition was determined by using linear regression to extrapolate the I_0/E_0 ratio, resulting in complete enzyme inhibition. (C) The interaction of catG with SRP-3 was assessed under second-order conditions. Equimolar amounts of SRP-3 and catG were incubated at 25 °C for varying periods of time (0–30 min). The reaction was stopped by the addition of substrate (1 mM Z-Lys-SBzl and 250 μ M DTDP), and the velocity of free catG was measured using a microplate reader. Velocity was converted to free enzyme concentration using an enzyme concentration standard curve. The k_a for the SRP-3–catG interaction in this representative experiment was $1.3 \times 10^5 \text{ M}^{-1} \text{ s}^{-1}$. (D) Inhibition of chymotrypsin under pseudo-first-order conditions. Human chymotrypsin (10 nM) and the substrate Succ-AAPF-pNA (1 mM) were added to SRP-3 at 0 (\square), 160 (+), 240 (\blacktriangle), 360 (\triangle), 480 (\times), and 640 nM (\circ). The progress of the inactivation of the enzyme at each concentration of serpin was followed by measuring the change in absorbance (OD₄₀₅) every 15 s (inset). Assuming an irreversible reaction, the first-order rate constants (k_{obs}) were calculated by a nonlinear regression fit of each curve. The k_{obs} values were plotted against the inhibitor concentration, and the slope of this line was used to determine the second-order rate constant (k'). By accounting for the K_m of the enzyme for the substrate, we calculated a corrected second-order rate constant (k_a). The k_a for the SRP-3–chymotrypsin interaction in this representative experiment was $0.7 \times 10^5 \text{ M}^{-1} \text{ s}^{-1}$.

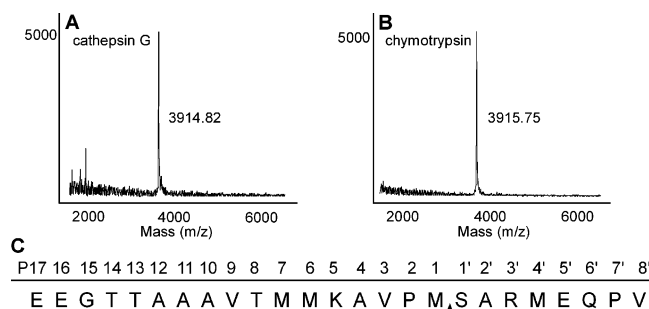


FIGURE 5: Reactive center of SRP-3. GST–SRP-3 protein (30 μ g) was mixed with catG (1 μ g) or chymotrypsin (1 μ g) and incubated for 15 min at 25 °C. The reaction mixture was then analyzed by MALDI-MS. (A) Molecular mass of the catG-cleaved fragment. (B) Molecular mass of the chymotrypsin-cleaved fragment. (C) Reactive site loop of SRP-3 showing the location of the catG and chymotrypsin cleavage site (black arrowhead) deduced from the MALDI-MS data.

2.2 kb of the upstream promoter sequence, in-frame into the *LacZ* pPD95.10 expression vector (a kind gift from A. Fire). The *srp-3::lacZ* transgene was injected into young hermaphrodites along with a *myo-3::gfp* co-injection marker to identify transgenic progeny. Stable lines expressing *myo-3::gfp* were enriched and stained with X-gal to visualize *srp-3*-directed *lacZ* expression. No SRP-3::*lacZ* expression was

evident during embryogenesis (data not shown). However, SRP-3 expression was visible in all stages of the nematode postembryonic development (Figure 6A). In the early larval (L2) stage, *lacZ* staining was noticeable in the posterior intestinal and anterior muscle cells (Figure 6B). In the late larval (L4) to adult stages, *lacZ* staining can be seen in the body wall muscles, particularly in the anterior region of the worm (Figure 6C,D). To visualize SRP-3 expression in live, intact animals, transgenic animals expressing *srp-3::gfp* fusion constructs also were generated. Consistent with the *lacZ* data, *srp-3*-directed GFP expression was evident throughout postembryonic development. However, expression was restricted primarily to the anterior muscle cells (Figure 6E,F).

DISCUSSION

Serpins_{IC} have been detected in all domains of life. Despite their widespread distribution, the biological functions of serpins_{IC} in the context of an intact organism have been difficult to ascertain. Reverse genetic strategies using mice have been confounded by the relatively large copy number of serpins_{IC} in the genome, as well as their overlapping expression patterns and inhibitory profiles (16–20). Due to these limitations, we sought to determine whether a simpler multicellular organism with a smaller serpin_{IC} repertoire

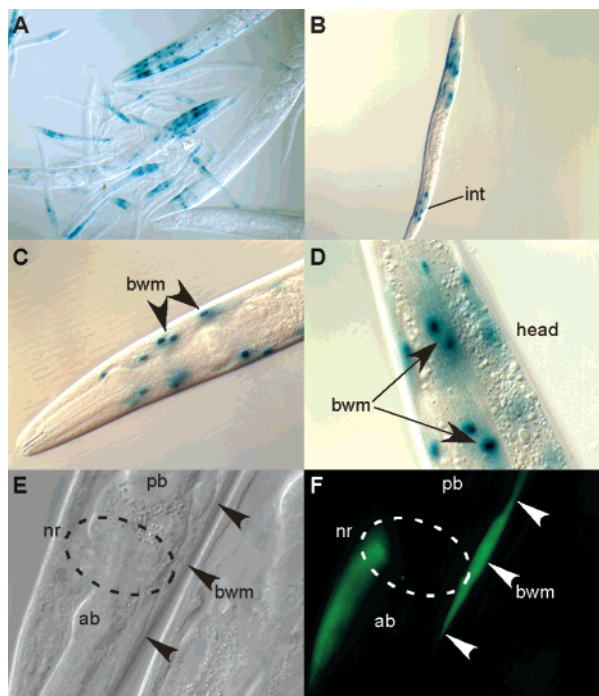


FIGURE 6: SRP-3 expression pattern. Lines of transgenic *C. elegans* carrying the SRP-3::lacZ (or GFP) reporter gene were generated by gonadal injection. (A) SRP-3::lacZ expression was visible in all postembryonic developmental stages of the worm. (B) SRP-3::lacZ expression in the posterior intestine and anterior muscle cells of the L2 stage larva. (C) Anterior region of a L4 larva showing lacZ expression in the body wall muscles (bwm, black arrowheads). (D) Strong SRP-3 expression in the body wall muscles of an adult hermaphrodite (black arrows). Higher-magnification photomicrographs using Normarski optics (E) and fluorescence microscopy (F) of the adult head. Note GFP expression in the anterior muscle cell (white arrowheads) near the nerve ring (dashed oval). Abbreviations: int, intestine; bwm, body wall muscle; ab, anterior bulb; pb, posterior bulb; nr, nerve ring.

might provide a more tractable approach. To this end, we initiated a comprehensive analysis of *C. elegans* serpin_{IC} activity.

The *C. elegans* genome contains nine serpin_{IC} genes that encode detectable RNA transcripts (4, 5). By computational assessment, only the SRP-1, -2, -3, -6, and -7 mRNAs should translate into full-length proteins with RSL amino acid residues suggestive of peptidase inhibitory-type serpins (4, 5). These studies confirmed that recombinant SRP-3 was a potent inhibitor of chymotrypsin-like, but not elastase-like, serine peptidases. In part, these findings were surprising as SRP-3 contained amino acid residues in its reactive center (P1–P1', Met-Ser) that were identical to those of α 1-antitrypsin (SERPINA1). Since the P1 residue is the primary determinant of serpin specificity in terms of target serine peptidases, we would have predicted that SRP-3, like α 1-antitrypsin, would have neutralized both chymotrypsin- and neutrophil elastase-like enzymes (21, 22). The inability of SRP-3 to neutralize neutrophil elastase suggested that residues more proximal or distal in the RSL (e.g., the P5 and P3' residues of SRP-3 are markedly different from those of α 1-antitrypsin; see Figure 2) might also affect binding specificities. Alternatively, since human neutrophil elastase, rather than nematode elastases, was used in the kinetic analysis, a poor fit may have generated an acyl–enzyme intermediate that was preferentially shuttled down the

substrate instead of the inhibitory pathway, thereby obscuring neutralizing activity (15). Regardless of whether SRP-3 can actually inhibit any type of elastase, these kinetic studies underscore the need to assess serpin activity experimentally and not to rely on inferences based on computer alignment similarities with other well-studied serpins.

The finding that SRP-3 is an inhibitor of chymotrypsin-like serine peptidases confirmed that at least two of the five predicted *C. elegans* inhibitory-type serpins_{IC} could serve as functional inhibitors. In addition, SRP-3 was expressed predominately in both larval and adult muscle cells. In a previous study, we showed that SRP-2 was a dual cross-class inhibitor of granzyme B-like serine peptidases and papain-like cysteine peptidases and that this inhibitor was expressed in intestinal and hypodermal cells (5). Thus, these two serpins_{IC} complement one another by extending the family's overall inhibitory profile and tissue expression pattern in *C. elegans*. Interestingly, SRP-3 in *C. elegans* and SERPINB6 in humans both inhibit chymotrypsin-like enzymes and are expressed in muscle (<http://www.ncbi.nlm.nih.gov/entrez/query.fcgi?db=unigene>). Also, SRP-2 and SERPINB9 inhibit granzyme B and are expressed in skin (hypoderm) and some types of intestinal cells (<http://www.ncbi.nlm.nih.gov/entrez/query.fcgi?db=unigene>). Thus, there would appear to be some evolutionary conservation of tissue specific inhibitory function between early metazoans and mammals.

The expression of SRP-3 in muscle cells raises intriguing possibilities in terms of its proposed function in vivo. Loss of muscle mass occurs by peptidase- and non-peptidase-mediated pathways. Of the peptidase-mediated pathways, proteosomal and nonproteosomal mechanisms have been identified, and inhibition of these latter pathways, especially those involving serine peptidases, can lead to attenuation of muscle atrophy (23). The nonproteosomal, peptidase-mediated muscle degradation pathways in *C. elegans* are activated by the fibroblast growth factor (*egl-15*)/RAS (*let-60*)/MAP kinase (*mpk-1*) signaling cascade (24, 25). Thus, it will be interesting to determine whether loss-of-function mutations of *srp-3* accelerate muscle mass degradation in animals with constitutive activation of this pathway.

ACKNOWLEDGMENT

We thank David Hall at the Center for *C. elegans* Anatomy (sponsored by the National Institutes of Health Division of Research Resources) for assistance with worm anatomy and expression pattern analysis. We thank Andy Fire for providing lacZ and GFP expression vectors and Yuji Kohara for cDNA clones. The N2 worm strain was provided by the *C. elegans* Genetics Center (<http://biosci.umn.edu/CGC/Strains/request.html>).

REFERENCES

1. Pike, R. N., Buckle, A. M., le Bonniec, B. F., and Church, F. C. (2005) Control of the coagulation system by serpins. Getting by with a little help from glycosaminoglycans, *FEBS J.* 272, 4842–4851.
2. Silverman, G. A., Bird, P. I., Carrell, R. W., Coughlin, P. B., Gettins, P. G., Irving, J. I., Lomas, D. A., Luke, C. J., Moyer, R. W., Pemberton, P. A., Remold-O'Donnell, E., Salvesen, G. S., Travis, J., and Whisstock, J. C. (2001) The serpins are an expanding superfamily of structurally similar but functionally

- diverse proteins: Evolution, mechanism of inhibition, novel functions, and a revised nomenclature, *J. Biol. Chem.* 276, 33293–33296.
3. Silverman, G. A., Whisstock, J. C., Askew, D. J., Pak, S. C., Luke, C., Cataltepe, S., Irving, J. A., and Bird, P. I. (2004) Human clade B serpins (ov-serpins) belong to a cohort of evolutionarily-dispersed intracellular proteinase inhibitor clades that protect cells from promiscuous proteolysis, *Cell. Mol. Life Sci.* 61, 301–325.
 4. Luke, C. J., Pak, S. C., Askew, D. J., Askew, Y. S., Smith, J. E., and Silverman, G. A. (2006) Selective conservation of the rsl-encoding, proteinase inhibitory-type, clade I serpins in *Caenorhabditis* species, *Front. Biosci.* 11, 581–594.
 5. Pak, S. C., Kumar, V., Tsu, C., Luke, C. J., Askew, Y. S., Askew, D. J., Mills, D. R., Bromme, D., and Silverman, G. A. (2004) Srp-2 is a cross-class inhibitor that participates in post-embryonic development of the nematode *Caenorhabditis elegans*: Initial characterization of the Clade L serpins, *J. Biol. Chem.* 279, 15448–15459.
 6. Jameson, G. W., Roberts, D. V., Adams, R. W., Kyle, W. S., and Elmore, D. T. (1973) Determination of the operational molarity of solutions of bovine α -chymotrypsin, trypsin, thrombin and factor Xa by spectrofluorimetric titration, *Biochem. J.* 131, 107–117.
 7. Salvesen, G., and Nagase, H. (1989) Inhibition of proteolytic enzymes, in *Proteolytic enzymes: A practical approach* (Beynon, R. J., and Bond, J. S., Eds.) pp 83–104, IRL Press, Oxford, U.K.
 8. Schick, C., Kamachi, Y., Bartuski, A. J., Cataltepe, S., Schechter, N. M., Pemberton, P. A., and Silverman, G. A. (1997) Squamous cell carcinoma antigen 2: A novel serpin that inhibits the chymotrypsin-like proteinases cathepsin G and mast cell chymase, *J. Biol. Chem.* 272, 1849–1855.
 9. Morrison, J. F., and Walsh, C. T. (1988) The behavior and significance of slow-binding enzyme inhibitors, *Adv. Enzymol. Relat. Areas Mol. Biol.* 61, 201–301.
 10. Beatty, K., Bieth, J., and Travis, J. (1980) Kinetics of association of serine proteinases with native and oxidized α -1-proteinase inhibitor and α -1-antichymotrypsin, *J. Biol. Chem.* 255, 3931–3934.
 11. Schick, C., Pemberton, P. A., Shi, G.-P., Kamachi, Y., Cataltepe, S., Bartuski, A. J., Gornstein, E. R., Bromme, D., Chapman, H. A., and Silverman, G. A. (1998) Cross-class inhibition of the cysteine proteinases cathepsins K, L, and S by the serpin squamous cell carcinoma antigen 1: A kinetic analysis, *Biochemistry* 37, 5258–5266.
 12. Lewis, J. A., and Fleming, J. T. (1995) Basic culture methods, *Methods Cell Biol.* 48, 3–29.
 13. Fire, A., Harrison, S. W., and Dixon, D. (1990) A modular set of *lacZ* fusion vectors for studying gene expression in *Caenorhabditis elegans*, *Gene* 93, 189–198.
 14. McKay, S. J., Johnsen, R., Khattra, J., Asano, J., Baillie, D. L., Chan, S., Dube, N., Fang, L., Goszczynski, B., Ha, E., Halfnight, E., Hollebakken, R., Huang, P., Hung, K., Jensen, V., Jones, S. J., Kai, H., Li, D., Mah, A., Marra, M., McGhee, J., Newbury, R., Pouzyrev, A., Riddle, D. L., Sonnhhammer, E., Tian, H., Tu, D., Tyson, J. R., Vatcher, G., Warner, A., Wong, K., Zhao, Z., and Moerman, D. G. (2003) Gene expression profiling of cells, tissues, and developmental stages of the nematode *C. elegans*, *Cold Spring Harbor Symp. Quant. Biol.* 68, 159–169.
 15. Gettins, P. G. (2002) Serpin structure, mechanism, and function, *Chem. Rev.* 102, 4751–4803.
 16. Dougherty, K. M., Pearson, J. M., Yang, A. Y., Westrick, R. J., Baker, M. S., and Ginsburg, D. (1999) The plasminogen activator inhibitor-2 gene is not required for normal murine development or survival, *Proc. Natl. Acad. Sci. U.S.A.* 96, 686–691.
 17. Scarff, K. L., Ung, K. S., Nandurkar, H., Crack, P. J., Bird, C. H., and Bird, P. I. (2004) Targeted Disruption of SPI3/Serpinb6 Does Not Result in Developmental or Growth Defects, Leukocyte Dysfunction, or Susceptibility to Stroke, *Mol. Cell. Biol.* 24, 4075–4082.
 18. Kaiserman, D., Knaggs, S., Scarff, K. L., Gillard, A., Mirza, G., Cadman, M., McKeone, R., Denny, P., Cooley, J., Benarafa, C., Remold-O'Donnell, E., Ragoussis, J., and Bird, P. I. (2002) Comparison of human chromosome 6p25 with mouse chromosome 13 reveals a greatly expanded ov-serpin gene repertoire in the mouse, *Genomics* 79, 349–362.
 19. Askew, D. J., Askew, Y. S., Kato, Y., Luke, C. J., Pak, S. C., Bromme, D., and Silverman, G. A. (2004) The amplified mouse squamous cell carcinoma antigen gene locus contains a serpin (serpinb3b) that inhibits both papain-like cysteine and trypsin-like serine proteinases, *Genomics* 84, 166–175.
 20. Askew, D. J., Askew, Y. S., Kato, Y., Turner, R. F., Dewar, K., Lehoczy, J., and Silverman, G. A. (2004) Comparative genomic analysis of the clade B serpin cluster at human chromosome 18q21: Amplification within the mouse squamous cell carcinoma antigen gene locus, *Genomics* 84, 176–184.
 21. Duranton, J., Adam, C., and Bieth, J. G. (1998) Kinetic mechanism of the inhibition of cathepsin G by α 1-antichymotrypsin and α 1-proteinase inhibitor, *Biochemistry* 37, 11239–11245.
 22. Johnson, D., and Travis, J. (1979) The oxidative inactivation of human α -1-proteinase inhibitor. Further evidence for methionine at the reactive center, *J. Biol. Chem.* 254, 4022–4026.
 23. Morris, C. A., Morris, L. D., Kennedy, A. R., and Sweeney, H. L. (2005) Attenuation of skeletal muscle atrophy via protease inhibition, *J. Appl. Physiol.* 99, 1719–1727.
 24. Szewczyk, N. J., and Jacobson, L. A. (2003) Activated EGF-15 FGF receptor promotes protein degradation in muscles of *Caenorhabditis elegans*, *EMBO J.* 22, 5058–5067.
 25. Szewczyk, N. J., Peterson, B. K., and Jacobson, L. A. (2002) Activation of Ras and the mitogen-activated protein kinase pathway promotes protein degradation in muscle cells of *Caenorhabditis elegans*, *Mol. Cell. Biol.* 22, 4181–4188.

BI052626D